NbN Hot-Electron-Bolometer Mixer for Operation in the Near-IR Frequency Range

Yury Lobanov, Michael Shcherbatenko, Matvey Finkel, Sergey Maslennikov, Alexander Semenov, Boris M. Voronov, Alexander V. Rodin, Teunis M. Klapwijk, and Gregory N. Gol'tsman

***Abstract*—Traditionally, hot-electron-bolometer (HEB) mixers are employed for THz and "super-THz" heterodyne detection. To explore the near-IR spectral range, we propose a fiber-coupled NbN film based HEB mixer. To enhance the incident-light absorption, a quasi-antenna consisting of a set of parallel stripes of gold is used. To study the antenna effect on the mixer performance, we have experimentally studied a set of devices with different size of the Au stripe and spacing between the neighboring stripes. With use of the well-known isotherm technique we have estimated the absorption efficiency of the mixer, and the maximum efficiency has been observed for devices with the smallest pitch of the alternating NbN and NbN-Au stripes. Also, a proper alignment of the incident $\vec{E}$-field with respect to the stripes allows us to improve the coupling further. Studying *IV*-characteristics of the mixer under differently-aligned $\vec{E}$-field of the incident radiation, we have noticed a difference in their shape. This observation suggests that a difference exists in the way the two waves with orthogonal polarizations parallel and perpendicular $\vec{E}$-field to the stripes heat the electrons in the HEB mixer. The latter results in a variation in the electron temperature distribution over the HEB device irradiated by the two waves.**

***Index Terms*—Hot-electron-bolometer mixer, optical antenna, optical heterodyne detection, polarization-sensitive detection.**

I. Introduction

FOR over a decade, superconducting NbN hot-electron-bolometer (HEB) mixers have shown excellent performance at frequencies above the gap-frequency of the superconductor [1]–[4]. Since the conversion efficiency of the HEB mixer does not degrade with increasing frequency until the plasma frequency of the metal is achieved, it is quite promising to explore the performance of these mixers at even higher frequencies than reported so far. Development of the HEB mixer for the near-IR frequency range is potentially beneficial for astrophysical observations, where power detection with high sensitivity and resolution will allow precise profile measurement of spectral lines and quantum applications, such as quantum optical tomography [5], [6], optical coherent tomography [7], or distributed fiber-optic sensing [8]. On the other hand, pumping the HEB mixer with IR radiation presents an interesting scientific subject in itself, because it is the first attempt to evaluate the HEB mixer performance and response to radiation at a frequency of ∼200 THz. We reported recently the development and initial characterization of a heterodyne receiver with a fiber-coupled HEB mixer with a Distributed-Feedback (DFB) laser acting as a Local Oscillator (LO) at a wavelength of 1.55 micrometers [9]. In general, such a mixer could be made of a NbN film of the same area as the fiber core counting on the direct absorption of the incident light in the film. This approach possesses two drawbacks. First, a significant LO power is needed to pump the mixer to its optimal bias point and, second, the mixer conversion efficiency is limited by the absorption efficiency of the NbN film. To overcome these issues, we have introduced an optical quasi-antenna which helps us both to reduce the LO power required and to improve light coupling to the mixer. This quasi-antenna consists of a set of equally spaced gold stripes on top of the NbN film. The antenna efficiency is strongly determined by the geometry of the stripes.

In this paper we present an experimental study of the incident-light coupling and the dependence of the power absorption on the size of the Au stripe and spacing between the stripes, as well as on the alignment of the incident radiation $\vec{E}$-field with respect to the stripes.

Manuscript received August 12, 2014; accepted November 14, 2014. Date of publication November 26, 2014; date of current version February 6, 2015. This work was supported in part by the Ministry of Education and Science of the Russian Federation, Contract No. 14.B25.31.0007, by Grant 11.G34.31.0074, and by the Russian Federation President Grant for Leading Scientific Schools #1918.2014.2. The work of M. Finkel and M. Shcherbatenko was supported by the Ministry of Education and Science of the Russian Federation under State Contract No. 3.2575.2014/κ, and A. S.—under State Contract No. 2327.

Y. Lobanov, M. Shcherbatenko, and A. Semenov are with the Moscow State Pedagogical University, 119571 Moscow, Russia, and also with the Moscow Institute of Physics and Technology, 141700 Dolgoprudny, Russia (e-mail: ylobanov@rplab.ru).

M. Finkel, S. Maslennikov, and B. M. Voronov are with the Moscow State Pedagogical University, 119571 Moscow, Russia.

A. V. Rodin is with the Moscow Institute of Physics and Technology (State University), 141700 Dolgoprudny, Russia, and also with the Space Research Institute, Russian Academy of Sciences, 117342 Moscow, Russia.

T. M. Klapwijk is with the Kavli Institute of NanoScience, Faculty of Applied Sciences, Delft University of Technology, 2628 CJ Delft, The Netherlands, and also with the Moscow State Pedagogical University, 119571 Moscow, Russia.

G. N. Gol'tsman is with the Moscow State Pedagogical University, 119571 Moscow, Russia, and also with the National Research University Higher School of Economics, 101000 Moscow, Russia.

Color versions of one or more of the figures in this paper are available online at http://ieeexplore.ieee.org.

Digital Object Identifier 10.1109/TASC.2014.2376191

II. Device Layout and Characterization

A. HEB Mixer Integrated With Optical Quasi-Antenna

The mixers are made of a 3.5 nm −20 nm thick NbN −Au bilayer-film deposited on a sapphire substrate in an *in situ* process. Technological details are given in [9]. Parameters of the devices are given in Table I. The use of fiber optics allowed us to align the LO and test signals easily with a fiber beam-splitter and to couple radiation directly to the NbN bridge measuring 7 μm × 7 μm. To enhance radiation absorption by

TABLE I
PARAMETERS OF THE DEVICES

Parameter	Device 1	Device 2	Device 3	Device 4
Number of stripes (NbN × NbN-Au)	1 × 0	3 × 2	29 × 30	39 × 40
Stripe length,* μm (NbN / NbN-Au)	7.0 × 0	0.4/2.9	0.06 / 0.18	0.08/0.1
Transition temperature, NbN / NbN-Au, K	10.0/8.5	11.4/10.4	13.0/12.05	7.0/6.5
Transition width, NbN / NbN-Au, K	0.8/0.1	0.3/0.8	0.5/0.1	0.9/0.1
Critical current, μA	2150	1700	1900	380
Critical current density, A/cm^2	7.7*10^6	6.1*10^6	6.0*10^6	1.4*10^6
Absorption efficiency, % polarizer is set to minimize pumping power, $\vec{E}$ is parallel to the stripes, ($\overrightarrow{E_\parallel}$)	7	6	7	14
Absorption efficiency, % polarizer is set to maximize pumping power, $\vec{E}$ is perpendicular to the stripes, ($\overrightarrow{E_\perp}$)		11	15	27

*Note, that term "length" is applied to a smaller dimension of a stripe, which corresponds to the bias current propagation trough the device.

the NbN film, a resonating or quasi-optical antenna structure is needed. Examples of optical antennas are given in [10]–[14].

Structures employing a surface plasmon resonance have been proposed as well [15]–[17]. An RF or THz antenna may be designed as scaled versions of their low-frequency prototypes, but this is not a valid solution for the optical range. To design an optical antenna, an effective wavelength λ_{eff} must be used to determine the geometry of the antenna, and as has been shown by Novotny [18] it should be in the range $\lambda/6 \leq \lambda_{\text{eff}} \leq \lambda/2$. Considering a single Au stripe as an antenna element we estimated a required size of about 60–220 nm [9]. We used a 20-nm-thick gold layer to form a set of alternating NbN and NbN–Au stripes by selectively removing the gold. A schematic view and SEM photographs of the devices are shown in Fig. 1.

B. Absorption Efficiency of the HEB Mixers

Fig. 2 shows a schematic of the experimental set-up used to study the HEB current-voltage characteristics and to measure the dependence of the absorption efficiency on the stripe geometry and incident-light polarization. We used a single-mode linearly polarized (1:6) fiber-coupled Distributed-Feedback laser operating at 1.55 μm. A Thorlabs polarization controller [19] was used to set the $\vec{E}$-vector orientation of the laser signal. A mechanical fiber-coupled attenuator was used to attenuate the laser power. The HEB mixer was installed on top of the fiber core, with an optical microscope to perform the alignment.

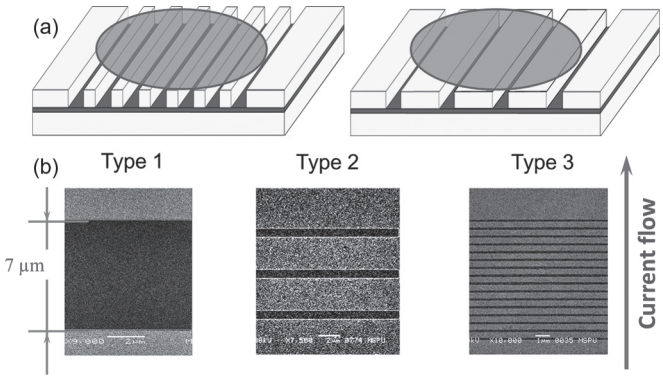

Fig. 1. A schematic view and SEM photographs of the devices. (a) Two examples of the gold stripe patterns are shown. The circle represents the device area aligned with the fiber core. (b) SEM photos of the three types of the devices. For type 1, the square NbN bridge and partly small contact pads are shown, for types 2 and 3, the pattern of stripes of gold and partly small contact pads are shown.

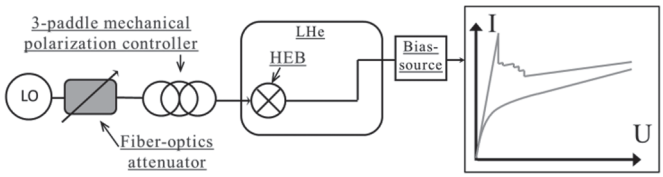

Fig. 2. A schematic of the experimental setup for measuring current-voltage dependence. A mechanical fiber-optics attenuator is used to vary the LO power and a mechanical polarization controller is used to align the $\vec{E}$-field. For biasing the mixer we used a voltage source.

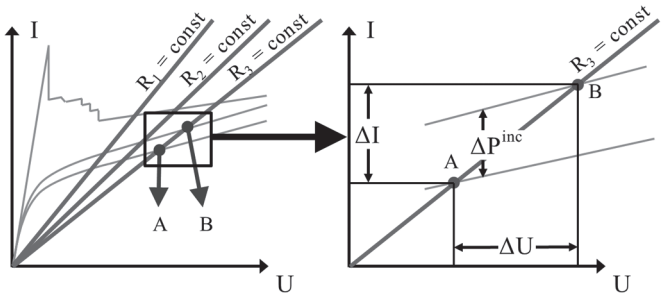

Fig. 3. A schematic representation of the isotherm method.

Pumping the device with a fixed orientation of the field $\vec{E}$, we were able to estimate the absorption efficiency of the mixers with the help of the isotherm method [20].

The method (Fig. 3) is based on the assumption that the DC resistance of the device depends on the electron temperature which increases linearly with the dissipated power. Also, heating the device by DC power and by incident power are considered to be equivalent. The latter is only true for high bias voltages where a large uniform hot spot is formed and the device is in the (quasi-)normal state [21].

Hence, for a given resistance the electron temperature and dissipated power are constant with no dependence on the origin of the dissipated power (applied DC bias or incident radiation).

For this reason, for any two bias points such that $\mathrm{U}_1/\mathrm{I}_1 = \mathrm{U}_2/\mathrm{I}_2$ and known incident power for the same bias points P_1^{inc} and P_2^{inc} one can estimate both absorbed power by the HEB mixer and absorption efficiency. From $\mathrm{I}_1 U_1 + P_1^{absorbed} = I_2 U_2 + P_2^{absorbed}$ and with another assumption that $P_1^{absorbed}/P_2^{absorbed} = P_1^{inc}/P_2^{inc}$ we found $P_2^{absorbed} =$

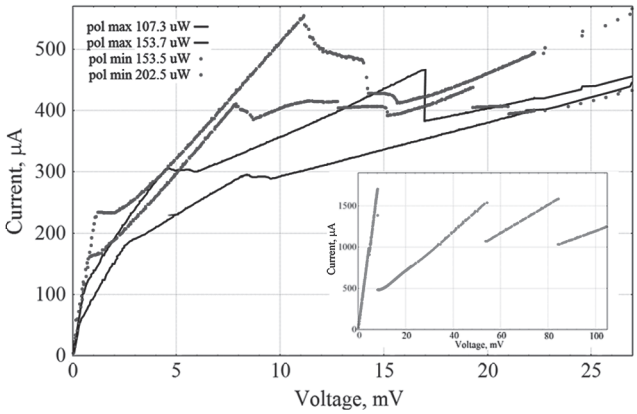

Fig. 4. Current-voltage characteristics of device #2 under differently polarized incident power set by the polarization controller. Pol max (lines) and pol min (dots) correspond to the polarization controller set to maximize and minimize pumping power, respectively. Inset shows the unpumped *IV*-curve.

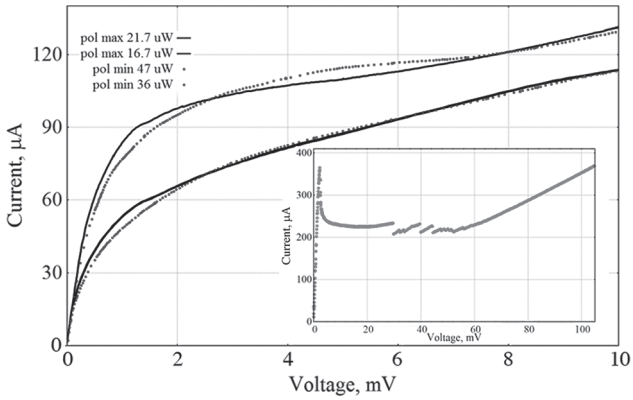

Fig. 5. Current-voltage characteristics of device #4 under differently polarized incident power set by the polarization controller. Pol max (lines) and pol min (dots) correspond to the polarization controller set to maximize and minimize pumping power, respectively. Inset shows the unpumped *IV*-curve.

$(U_2I_2-U_1I_1)/(P_1^{inc}/P_2^{inc}-1)$. And, hence, the absorption efficiency is simply $eff=P_2^{absorbed}/P_2^{inc}$. Using this technique, we estimated the absorption efficiency for both laser polarizations independently. Note that this calculation is only valid if no change of the laser polarization is made during the measurement and the accuracy of this method is determined by the assumptions made. The obtained results are in line with the HEB-mixer performance measurement [9]. Table I summarizes results obtained for different devices. With an increasing number of Au stripes (i.e. decreasing the individual stripe length) the absorption efficiency increases. The measured absorption efficiency for devices #3 and #4 is significantly improved compared to the mixer with a plain square NbN bridge.

C. Current-Voltage Characteristics of the HEB Mixer Under 1.5 μm Drive

By varying the applied LO power with a fiber-optical attenuator families of voltage-current characteristics were recorded. We notice a significant difference in the DC response of the devices when turning the vector $\vec{E}$ by 90°. The DC response of a given device to the near-IR applied radiation was found to be different depending on the (1) type of the device investigated and (2) polarization of the electrical field with respect to the position of the Au stripes on top of the superconducting bridge. Device with no Au stripes on top of the NbN bridge (device #1) responds to incident radiation independently on the settings of the polarization controller proving that the NbN bridge itself has no polarization sensitivity at all. *IV*-curves in this case are similar to those of a typical HEB obtained by applying radiation at frequencies higher than the energy gap of the superconducting material [22]. Gold stripes placed atop the NbN bridge cause the device to exhibit a number of critical currents which corresponds to the number of stripes in the pattern.

Applying Differently Polarized Radiation $\overrightarrow{\mathrm{E}_{\parallel}}$ and $\overrightarrow{\mathrm{E}_{\perp}}$ to a device with somewhat long NbN (0.4 μm) and NbN-Au (2.9 μm) stripes [device #2, Fig. 4] one can see that (1) the absorption efficiency strongly depends on the light polarization of the laser and (2) the alignment of the $\vec{\mathrm{E}}$-field also causes the shape of IV-curve to change in such a way that $I(V,P_{\perp}^{inc})$ is not a scaled version of $I(V,P_{\parallel}^{inc})$ anymore and cannot be achieved by adjusting the LO power only. This observation suggests that a difference exists in the way the two different waves (with parallel and perpendicular $\vec{\mathrm{E}}$-field to the stripes) heat the electrons in the HEB mixer.

Applying differently polarized radiation $\overrightarrow{\mathrm{E}_{\parallel}}$ and $\overrightarrow{\mathrm{E}_{\perp}}$ to a device with somewhat short NbN (0.06 or 0.08 μm) and NbN-Au (0.18 or 0.10 μm) stripes (device #3 and device #4 (Fig. 5)) one can also see that absorption efficiency strongly depends on the light polarization of the laser but the IV-curves show a similar shape with a negligibly small difference and $I(V,P_{\perp}^{inc})$ can be approached by adjusting incident power applied to *IV*-curve $I(V,P_{\parallel}^{inc})$. This observation suggests that the HEB mixer with a much shorter length of the stripes is heated more or less uniformly independently of the way the incident power is absorbed.

As is seen from Figs. 4 and 5, for devices with significantly different parameters of the stripes (i.e., the Au stripe size and spacing between the stripes) and the NbN film properties (critical temperature and current of the devices) we can deduce a phenomenological rule stating that a similar pumping level can be obtained if a device is irradiated by $\overrightarrow{\mathrm{E}_{\perp}}$ with incident power $\mathrm{P}_{\perp}^{\mathrm{inc}}$ or by $\overrightarrow{E_{\parallel}}$ with power $\mathrm{P}_{\parallel}^{\mathrm{inc}}=2\cdot\mathrm{P}_{\perp}^{\mathrm{inc}}$. This factor of 2 is also clearly seen from the data of Table I.

The measured bias current under LO power is the result of the DC bias voltage and the applied optical pumping. To reach a proper understanding of the observed response one needs a detailed analysis of the nonequilibrium state, the hot-electron state, for a non-uniform system in which the proximity effect plays a role. Such an investigation for a long superconducting strip terminated by the two bulk normal metal equilibrium reservoirs was carried out recently for a model system [23] which can be applied to a standard HEB.

In the model system, a nonuniform state of superconducting wire was observed with a maximum of the effective temperature in the middle of the strip and a double-peaked profile of superconducting gap [23]. In this case, one should take into account Andreev reflection which significantly complicates calculation of *IV*-curves.

For our devices we can also expect a multi-peaked temperature profile because of the non-uniformity of the temperature distribution over the bridge, caused by the difference in the

alternating NbN and NbN-Au stripes response to the incident power. The difference in the shape of the *IVs* set by applying differently polarized LO power (Fig. 4) suggests that the change in the $\vec{E}$-vector orientation causes a redistribution of the electron temperature over the NbN bridge. For power with $\vec{E}$-vector oriented perpendicular to the stripes, the absorption should mostly take place in the stripes with the higher impedance, i.e., in the NbN ones, leading to a temperature rise in the free-of-gold NbN stripes. For power with $\vec{E}$-vector oriented collinearly with the stripes the absorption should mostly take place in the stripes with the lower impedance at 200 THz, i.e., in the gold, leading to a temperature rise in the NbN-Au bilayer. For perpendicular orientation of the field the absorption is expected to be more efficient than for the collinear one. This is because the average sheet impedance [24] in the former case is determined by the free-of-gold NbN film and for all the investigated devices is of the order of the half-space impedance $\mathrm{Z}_0/2n$ (with $n = 1.54$ being the refractive index of the fiber and $\mathrm{Z}_0 = 377$ Ohm) and corresponds to good coupling of the film to the incident radiation. At the same time, the average impedance in the latter case is determined by the Au stripes and is of the order of only a few Ohms leading to significant reflection of the incident radiation.

A smaller difference in shape of *IVs* of the devices with shorter NbN and NbN-Au stripes (Fig. 4) indicates that a more uniform temperature distribution exists in this case.

III. Conclusion

In conclusion, we have integrated an HEB mixer with a planar quasi-optical antenna, which has significantly improved the coupling of the IR radiation to the detector. The mixers have been tested at 1.5 μm with fiber-optics to guide and couple the radiation. The measured absorption and efficiency of the HEB mixer with a fiber-coupled DFB laser serving as the LO shows the influence of the NbN—NbN-Au pattern on the coupling improvement. The measured receiver performance [9] is in line with the results obtained in the THz frequency range. However, the polarization direction of the applied LO power causes a different distribution of the electron temperature over the superconducting structure. As a result, the current-voltage characteristics differ not only in the different pumping levels achieved, but also in their shape. A more detailed study may provide a better understanding of the light absorption by the NbN—NbN-Au patterned structures. This is important both for understanding the cooling mechanisms of the thin film and bilayer-based superconducting structures and modeling and development of plasmonic antennas which play an important role in the optics and are being studied extensively for various applications.

References

[1] G. N. Gol'tsman, "Hot electron bolometric mixers: New terahertz technology," *Infrared Phys. Technol.*, vol. 40, no. 3, pp. 199–206, Jun. 1999.

[2] D. Meledin *et al.*, "A 1.3-THz balanced waveguide HEB mixer for the APEX telescope," *IEEE Trans. Microw. Theory Techn.*, vol. 57, no. 1, pp. 89–98, Jan. 2009.

[3] W. Zhang *et al.*, "Quantum noise in a terahertz hot electron bolometer mixer," *Appl. Phys. Lett.*, vol. 96, no. 11, Mar. 2010, Art. ID. 111113.

[4] I. Tretyakov *et al.*, "Low noise and wide bandwidth of NbN hot-electron bolometer mixers," *Appl. Phys. Lett.*, vol. 98, no. 3, Jan. 2011, Art. ID. 033507.

[5] J. B. Altepeter, E. R. Jerey, and P. G. Kwiat, "Photonic state tomography," *Adv. Atomic, Mol., Opt. Phys.*, vol. 52, pp. 105–159, 2005.

[6] A. Lvovsky and M. Raymer, "Continuous-variable optical quantum state tomography," *Rev. Modern Phys.*, vol. 81, pp. 299–332, Mar. 2009, (also available: arXiv:quant-ph/0511044).

[7] S. Chinn, E. Swanson, and J. Fujimoto, "Optical coherence tomography using a frequency-tunable optical source," *Opt. Lett.*, vol. 22, no. 5, pp. 340–342, Mar. 1997.

[8] T. Chen, K. P. Chen, Q. Wang, B. Zhang, and R. Chen, "Fiber optic distributed sensing with active self-heating," in *Imaging Appl. Opt. Tech. Dig.*, Monterey, CA, USA, 2012, Paper STu3F.2.

[9] Y. Lobanov *et al.*, "Heterodyne detection at near-infrared wavelengths with a superconducting NbN hot-electron bolometer mixer," *Opt. Lett.*, vol. 39, no. 6, pp. 1429–1432, Mar. 2014.

[10] X. Hu, E. A. Dauler, R. J. Molnar, and K. K. Berggren, "Superconducting nanowire single-photon detectors integrated with optical nano-antennae," *Opt. Exp.*, vol. 19, no. 1, pp. 7–31, Jan. 2011.

[11] G. D. Boreman, "Infrared microantennas," *Proc. SPIE*, vol. 3110, pp. 882–885, 1997.

[12] P. Bharadwaj, B. Deutsch, and L. Novotny, "Optical antennas," *Adv. Opt. Photon.*, vol. 1, pp. 438–483, 2009.

[13] A. Kawakami, S. Saito, and M. Hyodo, "Fabrication of nano-antennas for superconducting infrared detectors," *IEEE Trans. Appl. Supercond.*, vol. 21, no. 3, pp. 632–635, Jun. 2011.

[14] F. Gonzalez, J. Alda, B. Ilic, and G. D. Boreman, "Infrared antennas coupled to lithographic Fresnel zone plate lenses," *Appl. Opt.*, vol. 43, no. 33, pp. 6067–6073, Nov. 2004.

[15] M. Piliarik and J. Homola, "Surface plasmon resonance (SPR) sensors: Approaching their limits?" *Opt. Exp.*, vol. 17, no. 19, pp. 16505–16517, Sep. 2009.

[16] M. W. Knight *et al.*, "Aluminum plasmonic nanoantennas," *Nano Lett.*, vol. 12, no. 11, pp. 6000–6004, 2012.

[17] F. W. Carter, D. F. Santavicca, and D. E. Prober, "A plasmonic antenna-coupled superconducting near-IR photon detector," *Opt. Exp.*, vol. 22, no. 18, pp. 22062–22071, Sep. 2014.

[18] L. Novotny, "Effective wavelength scaling for optical antennas," *Phys. Rev. Lett.*, vol. 98, Jun. 2007, Art. ID. 266802.

[19] [Online]. Available: http://www.thorlabs.com/newgrouppage9.cfm?objectgroup_id=343

[20] H. Ekström, B. Karasik, E. Kollberg, and S. Yngvesson, "Conversion gain and noise of Nb superconducting hot electron mixers," *IEEE Trans. Microw. Theory Techn.*, vol. 43, no. 4, pp. 938–947, Apr. 1995.

[21] H. Merkel *et al.*, "A hot spot mixer model for superconducting phonon-cooled HEB far above the quasiparticle bandgap," in *Proc. 10th Int. Symp. Space THz Techn.*, 1999, pp. 592–606.

[22] Y. Lobanov *et al.*, "Large-signal frequency response of an HEB mixer: From 300 MHz to terahertz," *IEEE Trans. Appl. Supercond.*, vol. 21, pt. 1, no. 3, pp. 645–648, Jun. 2011.

[23] N. Vercruyssen, T. G. A. Verhagen, M. G. Flokstra, J. P. Pekola, and T. M. Klapwijk, "Evanescent states and nonequilibrium in driven superconducting nanowires," *Phys. Rev. B*, vol. 85, Jun. 2012, Art. ID. 224503.

[24] P. Yeh, *Optical Waves in Layered Media*. Hoboken, NJ, USA: Wiley, 2005.